Accepted Manuscript

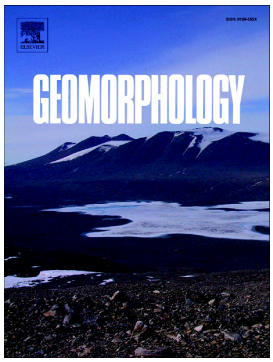

Distribution and characteristics of loess landslides triggered by the 1920 Haiyuan Earthquake, Northwest of China

Jianqi Zhuang, Jianbing Peng, Chong Xu, Zhenhong Li, Alexander Densmore, David Milledge, Javed Iqbal, Yifei Cui

PII: S0169-555X(17)30196-4
DOI: doi:10.1016/j.geomorph.2018.04.012
Reference: GEOMOR 6383

To appear in: *Geomorphology*

Received date: 3 May 2017
Revised date: 23 April 2018
Accepted date: 25 April 2018

Please cite this article as: Jianqi Zhuang, Jianbing Peng, Chong Xu, Zhenhong Li, Alexander Densmore, David Milledge, Javed Iqbal, Yifei Cui , Distribution and characteristics of loess landslides triggered by the 1920 Haiyuan Earthquake, Northwest of China. The address for the corresponding author was captured as affiliation for all authors. Please check if appropriate. Geomor(2017), doi:10.1016/j.geomorph.2018.04.012

Distribution and characteristics of loess landslides triggered by the 1920 Haiyuan Earthquake, Northwest of China

Jianqi Zhuang[a,b], Jianbing Peng[a*], Chong Xu[c], Zhenhong Li[b], Alexander Densmore[d], David Milledge[d], Javed Iqbal[e], Yifei Cui[f]

[a] College of Geological Engineering and Surveying of Chang'an University/Key Laboratory of Western China Mineral Resources and Geological Engineering, Xi'an 710054, China.

[b] COMET, School of Civil Engineering and Geosciences, Newcastle University, Newcastle upon Tyne NE1 7RU, UK.

[c] Institute of Geology, China Earthquake Administration, Beijing100029, China.

[d] Department of Geography, Durham University, Durham, DH1 3HP, UK

[e] Department of Earth Sciences, Abbottabad University of Sciences and Technology, Abbottabad, Pakistan

[f] Department of Civil and Environmental Engineering Hong Kong University of Science and Technology, Hong Kong, China

ABSTACT

On December 16, 1920, an earthquake with a magnitude of 8.5 occurred in Haiyuan County, Ningxia Hui Autonomous Region, Northwest of China. This earthquake triggered several thousand loess landslides which resulted in thousands of deaths and blockages of rivers. The distribution and characteristics of the landslides triggered by the Haiyuan Earthquake in loess areas were studied using satellite images and field investigation. A total of about 3,700 landslides with a cumulative area of about 177 km^2 were interpreted over an area of 21000 km^2.It was found that landslides triggered by the earthquake were concentrated in a western of 40-55 km from the

Haiyuan fault. Landslides were concentrated near ridge crests, with 65.7% of the landslides originating in the upper quadrant of slopes. The aspects of the landslides triggered by the Haiyuan Earthquake were parallel to the faults and there is no back-direction effect in landslides triggered by Haiyuan earthquake. These landslides have long run-out distances(travel distance (L) / height different (H) > 0.6) and deposited materials in river channels, forming 51 dammed lakes that still exist. The relationship between the area (A) and volume (V) of the landslides is $V=4.170\times A^{1.086}$. Based on the relationship between number and volume of landslide and the magnitude of earthquake, more than 100,000 landslides with a cumulative volume of $0.5\times10^{10}m^3$ were triggered by the Haiyuan Earthquake. As loess is sensitive to liquefaction during an earthquake and tends to produce landslides with long travel distances. Hence, the loess depth, slope and geological stresses are the primary factors responsible for the high density of landslides in this region.

Keywords

Coseismic loess landslide; Distribution; Characteristics; Haiyuan Earthquake

1. Introduction

Loess is distributed in arid and semi-arid regions and formed by the accumulation of wind-blown fine sand and clay components. The Loess Plateau has an area of approximately 430,000 km^2 and constitutes the main part of the loess area in China (Liu, 1985). The thickness of loess deposits in this area varies from few meters to more than 300 m (Derbyshire, 2000; Li et al., 2013). Loess is characterized by macro-pores, vertical joints, loose texture and silt content of more than 50%, which makes it sensitive to earthquakes and consequent landslides (Zhang and Wang,1995; Derbyshire, 2000; Dijkstra 1995; Xu et al., 2007; Zhang and Wang, 2007; Zhang et al., 2009; Zhuang et al., 2016). The Loess Plateau in China is located in the Orodos Block, which

is bounded by an active earthquake zone and many earthquakes with magnitudes of higher than 6.0 have been reported in this area, and most of the loess landslides in this area are known to have been triggered by historical earthquakes (Derbyshire, 1991;Li et al., 2009; Liu et al., 2015; Li et al.,2015). Some examples of strong earthquakes in this region include the Hongdong County Earthquake in 1303 (*Mw*= 8.0), Hua County Earthquake in 1556 (*Mw*=8.0), Tianshui City Earthquake in 1654 (*Mw*=8.0), Tongwei County Earthquake in 1718 (*Mw*=7.5), Haiyuan County Earthquake in 1920 (*Mw*=8.5), and Gulang County Earthquake in 1927 (*Mw*=8.0, Xie and Cai, 1983; 1985; 1987a, 1988b). Each of these earthquakes triggered more than 10,000 loess landslides with more than 40,000 casualties (Liu et al., 2003).

On December 16, 1920, a strong earthquake of *M*w 8.5 (Zhang et al., 1987) occurred in Haiyuan County, Ningxia Hui Autonomous Region, Northwest of China. This earthquake has been the focus of many studies (Zhang et al., 1987; Zhang et al., 1988a, 1988b; Zhang and Wang, 1995; Zhang and Wang, 2007; Zhang et al., 2009; Li et al., 2009; Liu et al., 2015; Li et al., 2015). The strongest quaking activity lasted for nearly 6 minutes (Zhang et al., 1987), with a seismic intensity of up to twelve degrees on the Chinese Seismic Intensity Scale in the meizoseismal area. About 500,000 houses and cave dwellings collapsed and a large number of houses were damaged to various extents (Seismological Institute of Lanzhou, SSB. and Seismological Team of Ningxia Hui Autonomous Region, 1980;Zhang et al., 1987). Altogether, 234,117 people died and many were injured (Seismological Institute of Lanzhou, SSB. and Seismological Team of Ningxia Hui Autonomous Region, 1980; Zhang and Wang,1995). Many of the earthquake-hit areas are covered by loess which is more sensitive to shake (Derbyshire 2000; Zhang and Wang 2007; Zhuang et al. 2017), which resulted in occurrence of thousands of landslides in the area. These landslides

blocked rivers, and buried farmland and villages (Seismological Institute of Lanzhou, SSB. and Seismological Team of Ningxia Hui Autonomous Region, 1980). An area of ~10,700 km^2 experienced a shaking intensity of ≥ ten and ~21,000 km^2 experienced an intensity of ≥ nine (Seismological Institute of Lanzhou, SSB. and Seismological Team of Ningxia Hui Autonomous Region, 1980).

Numerous studies have been done on landslides triggered by earthquakes; some of these studies established correlations between the environmental parameters of the slopes and landslides, influences of landform, earthquake magnitude, earthquake local geology, slope profiles, and vegetation cover, e.g., Wenchuan Earthquake occurrence in 2008 (Yin et al.,2009), Yushu Earquake occurrence in 2010 (Xu et al., 2013), Chi-Chi Earthquake occurrence in 1999 (Liao and Li, 2000; Lin and Tung, 2004), Northridge Earthquake occurrence in 1994 (Harp and Jibson, 1996), Kashmir Earthquake occurrence in 2005 (Owen et al., 2008). Other studies focused on the mechanism for slope failures triggered by earthquakes using dynamic triaxial test or shaking table test and simulated earthquake experiments (Wartmanet al., 2005; Lin and Wang, 2006; Wang and Lin,2011). Meanwhile, other studies focused on the assessment of landslides triggered by earthquakes and several models have been proposed in different areas, such as the Newmark model (Jibson, 1993; Jibson and Harp, 2000). However, the characteristics and distributions of the loess landslides triggered by the Haiyuan Earthquake have not been studied in depth. This is because of a scarcity in data available from that period. Zhang and Wang (1995) conducted field investigations in the earthquake affected areas and provided a general description of landslides and barrier lakes. Some other studies focused on the mechanism behind loess landslides or used individual watersheds to conduct case studies of landslide distribution (Zhang and Wang, 2007;

Wang et al., 2014). Nevertheless, the in-depth study about distribution of the loess landslide in meizoseismal area triggered by the Haiyuan earthquake in 1920, their characteristics and comparison with other earthquake-triggered landslides have not been done so far.

In this paper, we analyzed the distribution and characteristics of the landslides triggered by the Haiyuan Earthquake in 1920 based on image interpretation and field investigations. The spatial distribution of the landslides triggered by the earthquake was obtained by correlating with the influencing factors that control earthquake-triggered landslide occurrence eg, slope, aspect and distance to the fault, and the mechanisms behind their distribution and long run-out distances are discussed.

2. Study area

The area affected by the Haiyuan Earthquake is located along the northeastern margin of the Tibetan Plateau in the Ningxia-Hui Autonomous Region, Northwest of China (Figure 1). The earthquake occurred along the Haiyuan fault, which is an active left-lateral fault near the northeastern edge of the Tibetan Plateau (Burchfiel et al., 1991). The Haiyuan fault can be divided into eastern and western sections (Burchfiel et al., 1991). The western section branches of the Altyn Tagh fault in the Qilian Shan mountain range and continues eastward with a strike of around 110°. It then veers to a 140° strike east of the Yellow River and at the border of Haiyuan County (Burchfiel et al., 1991). The fault separates mountainous topography to the south with relief of up to 2900 m from low-relief areas to the north. The eastern fault zone exhibits an approximately ~155° strike and connecting it with the Liupanshan fault at the Liupanshan Mountains. Here, the fault separates bedrock and loess of the Liupanshan from loess tablelands and Quaternary sediments of the Guyuan Basin.

The M_w 8.5 Haiyuan Earthquake occurred at 20:06 on December 16, 1920 (Seismological Institute of Lanzhou, SSB. and Seismological Team of Ningxia Hui Autonomous Region, 1980; Zhang and Wang,1995). The epicenter of the earthquake was at Salt Lake (36.65° N, 105.29° E), 30 km west of Haiyuan County Town (Figure 1), with a focal depth of 26 km (Seismological Institute of Lanzhou, SSB and Seismological Team of Ningxia Hui Autonomous Region, 1980; Zhang and Wang, 1995). The strongest shaking lasted for around 6 min and produced a surface rupture extending along the Haiyuan fault from Salt Lake to Guyuan County (Zhang and Wang,1995), with a total distance of ~220 km. Coseismic surface rupture reached a maximum of about 10 m (Zhang et al., 1987).

Figure 1 The landform and epicenter of the 1920 Haiyuan Earthquake

Until 1923, there were six aftershocks with a magnitude of higher than 5; the strongest had a *Mw* of 7 and occurred on 25 Dec. 1920 (Seismological Institute of Lanzhou, SSB and Seismological Team of Ningxia Hui Autonomous Region, 1980; Burchfiel et al., 1991).

3. Landslide data and method

3.1 Landslide data

The earthquake produced intense shaking in a loess-covered area with high topographic relief which resulted in many earthquake-induced geohazards. The strong main quake and aftershocks as well as the large surface displacement triggered numerous landslides (Seismological Institute of Lanzhou, SSB. and Seismological Team of Ningxia Hui Autonomous Region, 1980), particularly in loess areas. In these areas, the landslides were characterized by a long travel distance(Zhang

and Wang, 2007; Wang et al., 2014). Although the Haiyuan Earthquake occurred nearly 100 years prior to this study, and the loess areas within the study area have undergone rapid erosion (Zhang et al., 1991; Shi and Shao, 2000), there is still observable evidence of large landslides which were observed during field investigations. In the loess-covered area, where quake intensities were more than seven degrees, the features of landslide scars and landforms can still be identified using satellite images (SPOT, with 5m resolution and obtained 2010-2015, Figure 2) and a Digital Elevation Model (DEM, with 25 m resolution obtained 1990s).The evidence support that these landslides were triggered by the Haiyuan Earthquake are follows:

Firstly, the local people from their father or grandfather information pointed that the landslides were triggered by the Haiyuan Earthquake in 1920. Secondly, the landslides belong to loess landslide and the area is covered by a great depth of loess which is very sensitive to water and the quick landform-change during rainy seasons, if the landslide were formed more than 300 years, they would have been changed and the features of the landslide would not be obvious (eg: the loess landslides triggered by the Tianshui City Earthquake in 1654 with magnitude *Mw* 8.0). Thirdly, there is no large earthquake (*Mw*>7) reported in the intensity of eight of the Haiyuan Earthquake hit-areas in 1920 nearly 700 years before 1920 (Zhang et al., 1987; Burchfie et al., 1991). So, we take the intensity of 8 of the Haiyuan Earthquake in 1920 as example to study the loess landslide triggered by earthquake, their distribution and characteristics. There are some large earthquake events outside intensity of 8 of the Haiyuan *Mw* in 1920, eg the Gulang Earthquake with the *Mw* of 8.0 in 1927, the Tongwei Earthquake with the *Mw* of 7.5 in 1718, the Tianshui Earthquake with the *Mw* of 8.0 in 1654 (Figure 3).

Figure 2 The typical landslides triggered by 1920 Haiyuan Earthquake and the features are still visible

Figure 3 The history of earthquakes and faults around the 1920 Haiyuan Earthquake

3.2 Method

Landslide data were obtained from image interpretation followed by field investigations. The landslides were interpreted from satellite images using the technique of the rear wall of landslide with the notable armchair-shaped features and texture of the dislocated or discontinued contour line. Landslide data include area, location, travel distance, and height difference which were obtained by a Portable Laser Range Measuring Instrument (PLRM) during site surveys.

Landslides were measured, from the nearest ridge (d_{top}) and the nearest stream (d_{st}) from DEMs using hydrology and near tools using ArcGIS. The measured distances were normalized by the total length of the slope (Meunier et al., 2008):

$$\left|d_{st,top}\right| = \frac{d_{st,top}}{d_{st} + d_{top}} \quad (1)$$

Where, the value of d_{st} varies from 0 for a cell located in the stream network to 1 for a ridge cell. The reverse is true for d_{top}.

Landslides located along the x-axis originated near or at a ridge crest, while landslides along the y-axis connected with a river channel. Landslides near the origin of the plot indicate that they moved from the ridge to the river channel, while landslides far from both axes were in a mid-slope position (Meunier et al, 2008).

We conducted soil tests on three loess soil samples from Xiji County following the standard

for Soil Test Method. Following the standards of China Method of Soil Test, the basic properties of the loess were measured. The cohesion and angle of internal friction were tested using the direct shear test method following soil test standard GBT50123-1999. The unit weight and porosity of the soil were measured using the Ring Sampler Method and bottle method.

4. Spatial distribution of coseismic landslides

4.1. Correlation between landslides and active faults

A total of 3,700 landslides were identified in this area (Figure 4). The landslides are distributed along the Haiyuan fault and mainly are concentrated along west of the fault, especially in the Xiji County.

Figure 4 Landslides identified as having been induced by the Haiyuan Earthquake in 1920

It is widely recognized that the active faults play an important role in determining landslide distribution during earthquakes. This is because the quake intensity and PGA (Peak Ground Acceleration) vary at different distances from the fault. Many studies have revealed that the landslides triggered by earthquakes tend to be clustered along the corresponding fault (Harp and Jibson, 1996; Keefer, 2000, 2002; Lin and Tung, 2004; Owen et al., 2008; Zhuang et al., 2010; Qi et al., 2010; Dai et al., 2011; Gorum et al., 2011; Cui et al., 2011), and become less numerous with increasing distance from the fault (Dai et al., 2011; Chen et al., 2017). Figure 5 indicates the frequency histogram of landslides occurring within every 5 km from the Haiyuan fault. The landslides were distributed primarily along the active faults of the main Haiyuan fault, but unlike in other earthquake events, there was no clear negative correlation between landslide number and

distance from the fault. Landslides were most prevalent in a zone that was 40-55 km from the Haiyuan fault.

Figure 5 The landslide distribution at different distances from the Haiyuan fault

Figure 6 Landslides distribution on both sides of the Haiyuan fault

Figure 6 shows the frequency histogram of landslides occurring within every 5 km from the Haiyuan fault differentiation between the western and eastern sides of the fault. The two sides of the main fault displayed dissimilar distributions. On the western of the fault, most landslides (433 per 5 km, on average) occurred in a zone 40-55 km from the fault. Beyond 55 km, the average was only 56 per 5 km. On the other hand, on the right side of the fault exhibited a more predictable pattern with fewer landslides being recorded with increasing distance from the fault. The average number of landslides per 5 km in the zones of 0-15km, 15-30 km and 30-50 km distant from the fault were 143, 124 and 35, respectively.

4.2. Landslide position on the slopes

Some researchers have pointed out that the landform can affect the PGA and amplified in ridges (Griffithsand Bollinger, 1979; Bouchonand Barker, 1996; Leeet al., 2008). As depicted in Figure 7, landslides were plotted to reveal the highest and lowest points of individual landslides in a frame of abscissa $|d_{top}|$ and ordinate $|d_{st}|$, and then associated with the area of a landslide by means of a circle with variable diameter. Landslides induced by the Haiyuan Earthquake (Figure 8) were clustered near ridge crests, with 65.7% of the landslides originating in the upper quadrant of slopes (normalized distance to ridge <0.4). This suggests that the upper parts of slopes are more

sensitive to earthquakes in loess areas. Further, 9.32% of these landslides with the $|d_{top}|$ and $|d_{st}|$ are 0, with the area of 0.22 km^2, this indicates that in some cases, entire slopes failed during the earthquake, and large landslides moved from ridges to stream channels with long travel distances.

Figure 7 Location of landslides with respect to ridge crest and stream.

Figure 8 Percentage of the landslide with respect to ridge crest.

4.3. Landslide distribution by aspect

Aspect can affect landslide occurrence during earthquakes due to the travel direction of earthquake waves (Huang and Li, 2008; Sato and Harp, 2009;Xu et al., 2011). The distribution of coseismic landslides follows the rules of the so-called "back slope effect" (Huang and Li, 2008; Sato and Harp, 2009;Xu et al., 2011), as evidenced by the Chi-Chi Earthquake in Taiwan (*M*w 7.6, 1999) and the Kashmir Earthquake in Pakistan (*M*w 7.6, 2005). According to the previous study, slopes facing the seismic source are less susceptible to landslides than the slopes parallel to the direction of travel as the earthquake waves (Huang and Li, 2008; Sato and Harp, 2009; Xu et al., 2011). The epicenter of the Haiyuan Earthquake was initially located in the western section of the fault and the rupture propagated southeast (Seismological Institute of Lanzhou, SSB. and Seismological Team of Ningxia Hui Autonomous Region, 1980; Burchfie et al., 1991; Zhang and Wang,1995). Figure 9 indicates that the landslide density on the northwest facing slopes (44.5%) was five times as that on the southeast slope (8.9%), while the area of the aspect of the slope distribution averagely in every facing. These observations differ from observations from other earthquakes (Huang and Li, 2008; Sato and Harp, 2009; Xu et al., 2011). The Haiyuan fault is a

strike-slip fault with left-lateral motion. The Chi-Chi, Kashmir, and Wenchuan Earthquakes were all thrust-fault earthquakes (Burchfie et al., 1991; Zhang and Wang,1995). The direction of movement of the main block is the primary determinant of landslide occurrence in a strike-slip fault (Huang and Li, 2008; Sato and Harp, 2009; Xu et al., 2011). Furthermore, slopes with aspects opposite to the direction of movement were more susceptible to landslides than other slope aspects in the Haiyuan Earthquake (Figure 10). Superposition of displacement to the doubling of the outward acceleration at the free boundary. The accelerate direction of the slope caused by the block move is different in the different aspect of the slope. The accelerate direction is according with the slope aspect which is the opposite to the block move direction and generate tensile stress in the slope. And the compressive stress generated in the slope along the block move direction. So, the slope which is the opposite to the block move direction is trend to failure due to tensile stress and the slope which is the opposite to the block move direction is not trend to failure due to compressive stress (Tang, 2008; Xu et al., 2011).

Figure 9 Location of landslides with respect to aspect.

Figure 10 Landslides after the 1920 Haiyuan Earthquake were easily induced at slopes facing the opposite direction from that of the movement of the block

5.Characteristics of landslides triggered by the Haiyuan Earthquake

5.1. Landslide size

The 1920 Haiyuan Earthquake triggered 3,700 landslides within the range of the intensity of 9-12,

with a total area of 177 km^2, over an area of about 21,000 km^2. The average landslide-point density and landslide-area density were 0.18 landslides/per km^2 and 0.85% respectively. Proportionally, the greatest number of landslides occurred to the southwest of the eastern section of the Haiyuan fault. As compared to the Wenchuan Earthquake, the landslide number, area, and density were lower in the Haiyuan Earthquake event (Harp and Jibson, 1996;Lin and Tung, 2004; Owen et al., 2008; Dai et al., 2011).

The mean landslide area was 0.048 km^2, which is greater than what is typical for landslides triggered by other earthquakes (Table 1). It is conceivable that some of the smaller landslides disappeared and were therefore not included in the analysis, thus raising the mean.

Table 1 The sizes and numbers of landslides triggered by earthquakes in recent years

We examined the area-frequency distribution of the earthquake event by log-log coordinates (Figure 11). The largest landslide was 0.4 km^2 and the cumulative number-area relationship for landslides can be represented as the logarithm of the number N of landslides exceeding a given area A. Higher values of the gradient may reflect poor efficiency in identifying small landslides and this distribution may be attributed to the fact that some small landslides were never identified due to soil erosion and human activity.

Figure 11 Landslide area cumulative frequency distribution

5.2. Travel distance

We examined the probability densities of equivalent coefficients of friction (landslide height

(*H*) / landslide travel distance (*L*)) for 31 rock landslides and 57 loess landslides triggered by earthquakes (Figure 12). Thirty-one rock landslides with long travel distances triggered by the 2008 Wenchuan Earthquake, were studied, including eleven datasets from the literature and 20 datasets from field investigations immediately after the earthquake (Zhang and Yin, 2013). The datasets included information on landslide height, travel distance and volume. Fifty-seven loess landslides triggered by the 1920 Haiyuan earthquake and the corresponding landslides were predominantly concentrated in a small watershed.

Figure 12 The probability densities of equivalent coefficients of friction

The *H*/*L* ratio of rock landslides triggered by earthquakes ranged from 0.1 to 0.75 with a mean of 0.42, while the loess landslides triggered by earthquakes ranged from 0.01 to 0.52 with a mean of 0.17.

The loess landslides induced by the earthquake were located in a different region of the graph from the rock landslides triggered by earthquake (Figure 13). The loess landslides move greater distances than rock landslides triggered by earthquakes, given an equivalent slope height. The relationship between the travel distance and equivalents lope height of the landslides induced by the Haiyuan Earthquake and Wenchuan Earthquake are $L = 8.308*H^{0.935}$ and $L = 4.117*H^{0.919}$. The best-fit curve for the former was much lower than the latter one. It indicates that the travel distance of loess landslides triggered by earthquake is much longer than rock landslides triggered by the Wenchuan earthquake at the same height.

Figure 13 The empirical relationship between landslide height and travel length

5.3. Geohazard chain due to long run-out distance landslides

Due to the landslides long travel distances and the deposition of landslide materials in major stream channels, several quake lakes formed in the areas affected by the Haiyuan Earthquake. Currently, 51 lakes are still present, primarily in southwestern Xiji County (Figure 14).

Figure 14 The quake lakes that formed after the Haiyuan Earthquake

Due to the human efforts for stabilization in the landslide-affected areas, the quake lakes became reservoirs for drinking water, agriculture, tourism and hydropower. Several urban settlements were constructed around the lakes, for example, Zhenhu (Quake lake)Township (Figure 15).

Figure 15 The group of quake lakes triggered by the Haiyuan Earthquake around Zhenhu (Quake lake) Township (Green box in Figure 14, the red rectangles are landslide dams)

6. Discussion

6.1. Area and number of landslides triggered by the Haiyuan Earthquake

We estimated total landslide volume (V) using a power-law landslide area-volume scaling relationship: $V=\alpha\times A^{\gamma}$, where α and γ are empirically-calibrated scaling parameters and A is the total landslide area. This is a widely used method to estimate landslide volume (Larsen et al. 2010). The area-volume relationship for landslides triggered by the Haiyuan Earthquake was obtained from field survey data. We investigated 89 well-preserved landslides to obtain and estimate their areas and mean depths, based on which the volume was calculated. Figure 16 depicts the relationship between the area and volume of the landslides induced by the Haiyuan Earthquake:

V=4.170×$A^{1.086}$. In general, the number of landslides triggered and landslides area is mainly affected by the magnitude of an earthquake (Xu et al., 2016; Havenith et al., 2016). However, the corresponding point for the Haiyuan Earthquake were located well below the regression line (Figure 17). The estimates of total volume of landslides which with the total area 177 km^2 associated with Haiyuan Earthquake was nearly 0.4×10^{10} m^3. This suggests that many landslides were not identified due to the long time lag and as a result, the actual number of landslides were probably underestimated. Based on historical data and analysis of the relationship between landslides and earthquake magnitude, we estimated that more than 100000 landslides with a total area of $0.5\times10^{10}m^3$ were triggered by the Haiyuan Earthquake (Figure 17). There are more than $0.1\times10^{10}m^3$ smaller landslide which were not identified due to loess rapid erosion and human activity.

Figure 16 Landslide number and area, and their correlations with earthquake magnitude (revised from Keefer, 2002)

6.2. Causes of the uneven landslide spatial distribution

The spatial landslide distribution of the Haiyuan Earthquake was atypical case as compared to other comparable earthquakes. Several hypotheses have since been proposed to improve understanding of landslide distribution (Zhang and Wang, 1995; Zhang and Wang, 2007; 2014; Li et al., 2015; Havenith et al., 2015). It is widely accepted that the larger landslides triggered by the Haiyuan Earthquake were primarily in loess (Lin and Wang, 2006; Zhang and Wang, 2007; Wang et al., 2014; Li et al., 2015). Figure 18 shows the loess depth distribution in this area, indicating that it was deepest in west of the study area. Considering this fact, it is a question mark that the

landslides were focused in only the southwest. This may be because the northwest landform is a gently sloping loess dome. In addition to this, the mountain ranges separate northwestern Xiji County from the Haiyuan fault. Therefore, the Haiyuan fault's strike follows the northeastern foot of the range, and the displacement triggered by the Haiyuan Earthquake was sharply attenuated by the mountain range. However, the absence of mountains between the Haiyuan fault and the loess areas to its southeast, paved the way for a greater number of landslides to occur in this area. Finally, the left block of the Haiyuan fault moved from northwest to southeast, indicating that stress was concentrated towards the southeastern section of the fault and paving way for a larger number of slope failures.

Figure 17 Loess depth distribution in the area affected by the 1920 Haiyuan Earthquake

6.3. Number of loess landslides with long travel distances

Loess is characterized by macro-pores, vertical joints, loose texture and quake sensitivity, which makes it prone to landslides (Derbyshire, 2000; Dijkstra, 1995; Xu et al., 2007; Zhang et al., 2009; Zhang and Liu, 2010). Loose loess soil can be easily liquefied during an earthquake, and this process is known as dynamic liquefaction. Ter-Stepanian (1998) suggested that flow-type loess landslides were triggered by high pore air pressure during a quake. Loess landslides were classified as a type of rapid soil flow by Keefer (1984). The widely used criteria for the liquefaction potential of fine particles were originally proposed by Wang(1979). Soil can undergo liquefaction if it meets two conditions: 1) particles finer than 0.005 mm comprise less than 20% of the total; and2) that the saturation water content (W_s) to liquid limit (W_L) ratio is greater than 0.9. We conducted soil tests on three loess soil samples from Xiji County (Table 2), the particles less

than 0.005 mm in diameter comprised 13%-14% of all particles, the liquid limit was between 28% and 29%, and the calculated water content of fully saturated samples was between 36% and 39%. Hence the W_s/W_L ratio was above 0.9 (values of 1.25, 1.37 and 1.27). This confirms that the loess in Xiji County is sensitive to liquefaction during earthquakes and is likely to produce landslides with long travel distances.

Table 2 Physical parameters of the loess in Xiji County

7. Conclusions

The 1920 M_w 8.5 Haiyuan Earthquake triggered 3,700 landslides in areas with shaking intensities of up to 9, with a cumulative area of 177 km^2, over an area of about 21,000 km^2. The average landslide size was 0.048 km^2. The landslides were concentrated in a zone 40-55 km from the Haiyuan fault. The distribution characteristics were not symmetrical around the fault, with the greatest landslide concentration occurring at a distance of 40-55 km from the fault on the western side, and on the eastern side the landslide concentration decreased with distance from the fault which is not similar with that triggered by other earthquakes.

Landslides induced by the Haiyuan Earthquake were clustered near ridge crests, with 65.7% originating in the upper 40% of slopes. Slopes oriented away from the direction of movement of the block were more susceptible to landslides than those oriented towards or perpendicular to the direction of movement and there is no back-direction effect in landslides triggered by Haiyuan earthquake. Co-seismic loess landslides run out distance is longer than rock landslides which gives an equivalent landslide crest height. Liquefaction is a possible explanation for long run-out and

our results are consistent with this explanation, suggesting that the loess in the study area is sensitive to liquefaction during an earthquake. The deposition of landslide materials into main river channels had resulted in the formation of 51 quake lakes in this region. According to historical records and analysis of the relationship between landslides and earthquake magnitude, we estimated that over 5,000 km^2 area in the study area has exposed to landslides, and 100,000 landslides have been directly or indirectly triggered by the earthquake.

Acknowledgements

We would like to express our gratitude to the two anonymous reviewers and the editor for their critical but constructive comments on the initial version of the manuscript which made the current-revised manuscript more valuable for the readers. This study was financially supported by the National Natural Science Foundation of China (Grant No. 41572272, 41661134015 and 41790444), and the Central University Founding of the Chang'an University (310826163503).

References

Bouchon, M., Barker, J.S., 1996, Seismic response of a hill: the example of Tarzana, California, B. Seismol. Soc. Am. 86, 66–72.

Burchfiel, B.C., Zhang, P., Wang, Y., Zhang, W., Song, F., Deng, Q., Molnar, P., Royden, L., 1991, Geology of the Haiyuan fault zone, Ningxia-Hui Autonomous Region, China, and its relation to the evolution of the northeastern margin of the Tibetan Plateau. Tectonics 10(6),1091-1110.

Chen, C. W., Iida, T., Yamada, R., Effects of active fault types on earthquake-induced deep-seated landslides: A study of historical cases in Japan. Geomorphology, 295, 680-689.

Cui, P., Chen, X.Q., Zhu, Y.Y., Su, F.H., Wei, F.Q., Han, Y.S., Liu, H.J., Zhuang, J.Q., 2011, The Wenchuan earthquake (May 12, 2008), Sichuan province, China, and resulting geohazards. Natural Hazards 56(1), 19-36.

Dai, F.C., Xu, C., Yao, X., Xu, L., Tu, X.B., Gong, Q.M., 2011, Spatial distribution of landslides triggered by the 2008 Ms 8.0 Wenchuan earthquake, China. Journal of Asian Earth Sciences 40(4), 883-895.

Derbyshire, E., Meng, X.M., Dijkstra, T.A., 2000, Landslides in the Thick Loess Terrain of North-West China. John Wiley & Sons Ltd, London.

Dijkstra, T.A., Rogers, C.D..F, van Asch, T.W.J., 1995, Cut slope and terrace edge failures in Malan loess, Lanzhou, PR China. In Proceedings of the XI ECSMFE conference, Copenhagen, 61-67.

Gorum, T., Fan, X., van Westen, C.J., Huang, R.Q., Xu, Q., Tang, C., Wang, G., 2011, Distribution pattern of earthquake-induced landslides triggered by the 12 May 2008 Wenchuan earthquake. Geomorphology 133(3), 152-167.

Griffiths, D.W., Bollinger, G.A., 1979, The effect of Appalachlan mountain topography on seismic waves. B. Seismol. Soc. Am. 69, 1081–1105.

Gutenberg, B., Richter, C., 1942, Earthquake magnitude, intensity, energy, and acceleration. Bulletin of the Seismological Society of America 32(3), 163-191.

Harp, E.L., Jibson, R.W., 1996, Landslides triggered by the 1994 Northridge, California, earthquake. Bulletin of the Seismological Society of America 86(1B), 319-332.

Havenith, H. B., Strom, A., Torgoev, I., Torgoev, A., Lamair, L., Ischuk, A., Abdrakhmatov, K., 2015, Tien Shan geohazards database: Earthquakes and landslides. Geomorphology, 249, 16-31.

Havenith, H. B., Torgoev, A., Braun, A., Schlögel, R., Micu, M., 2016, A new classification of earthquake-induced landslide event sizes based on seismotectonic, topographic, climatic and geologic factors. Geoenvironmental Disasters, 3(1), 6.

Huang, R.Q., Li, W.L., 2008 Research on development and distribution rules of geohazards induced by Wenchuan earthquake on 12th May,2008. Chinese Journal of Rock Mechanics and Engineering 27(12), 2585-2592. (In Chinese)

Hungr, O., Evans, S.G., Bovis, M.J., Hutchinson, J.N., 2001, A review of the classification of landslides of the flow type. Environmental & Engineering Geoscience 7(3), 221-238.

Jibson, R.W., 1993, Predicting earthquake-induced landslide displacements using Newmark's sliding block analysis. Transportation research record, 1411.

Jibson, R.W., Harp, E.L., Michael, J.A., 2000, A method for producing digital probabilistic seismic landslide hazard maps. Engineering Geology 58(3), 271-289.

Keefer, D.K., 1984. Landslides caused by earthquakes. Geol. Soc. Am. Bull. 95, 406-421.

Keefer, D.K., 2000, Statistical analysis of an earthquake-induced landslide distribution-the 1989 Loma Prieta, California event. Engineering geology 58(3), 231-249.

Keefer, D.K., 2002, Investigating landslides caused by earthquakes–a historical review. Surveys in geophysics 23(6), 473-510.

Lee, S.J., Chan, Y.C., Komatitsch, D., Huang, B.S., Tromp, J., 2008, Effects of realistic surface topography on seismic ground motion in the Yangmingshan region of Taiwan based upon the spectral-element method and LiDAR DTM, B. Seismol. Soc. Am. 99, 681–693.

Li, C., Zhang, P.Z., Yin, J., Min, W., 2009, Late Quaternary left-lateral slip rate of the Haiyuan fault, northeastern margin of the Tibetan Plateau. Tectonics 28(5), TC5010.

Li, T.L., Wang, C.Y., Li, P., 2013, Loess Deposit and Loess Landslides on the Chinese Loess Plateau. In Wang, F. et al. (eds.), Progress of Geo-Disaster Mitigation Technology in Asia, Environmental Science and Engineering, Springer-Verlag Berlin Heidelberg, 235-261.

Li, W., Huang, R., Pei, X. and Zhang, X., 2015, Historical Co-seismic Landslides Inventory and Analysis Using Google Earth: A Case Study of 1920 Ms 8. 5 Haiyuan Earthquake, China. In Engineering Geology for Society and Territory-Volume 2, Springer International Publishing, 709-712.

Liao, H.W., Lee, C.T., 2000, Landslides triggered by the Chi-Chi earthquake. In Proceedings of the 21st Asian conference on remote sensing, Taipei, Vol. 1, 2.

Lin, M.L., Tung, C.C., 2004, A GIS-based potential analysis of the landslides induced by the Chi-Chi earthquake. Engineering

Geology 71(1), 63-77.

Lin, M.L., Wang, K.L., 2006, Seismic slope behavior in a large-scale shaking table model test. Engineering Geology 86(2), 118-133.

Liu, B., Zhang, J., Wu, J., Guo, H., 2003, Reevaluating on casualty in the Haiyuan Ms 8.5 earthquake on December 16, 1920, Earthquake Res. China 19(4), 386-399.

Liu, T.S., 1985, Loess and the Environment. Science Press, Beijing. (In Chinese)

Liu, Z.J., Shao, Y., Klinger, Y., Xie, K., Yuan, D., Lei, Z., 2015, Variability in magnitude of paleo earthquakes revealed by trenching and historical records, along the Haiyuan Fault, China. Journal of Geophysical Research: Solid Earth, 120(12), 8304-8333.

Meunier, P., Hovius, N., Haines, J.A., 2008, Topographic site effects and the location of earthquake induced landslides. Earth and Planetary Science Letters, 275(3), 221-232.

Owen, L.A., Kamp, U., Khattak, G.A., Harp, E.L., Keefer, D.K., Bauer, M.A., 2008, Landslides triggered by the 8 October 2005 Kashmir earthquake. Geomorphology, 94(1), 1-9.

Qi, S., Xu, Q., Lan, H., Zhang, B., Liu, J., 2010, Spatial distribution analysis of landslides triggered by 2008.5. 12 Wenchuan Earthquake, China. Engineering Geology, 116(1), 95-108.

Sato, H.P., Harp, E.L., 2009, Interpretation of earthquake-induced landslides triggered by the 12 May 2008, M7.9 Wenchuan earthquake in the Beichuan area, Sichuan Province, China using satellite imagery and Google Earth. Landslides 6, 153-159.

Seismological Institute of Lanzhou, SSB and Seismological Team of Ningxia Hui Autonomous Region. Haiyuan great earthquake in 1920.Seismological press, Beijing 1980.

Shi, H., Shao, M., 2000, Soil and water loss from the loess plateau in china. Journal of Arid Environments 45(1), 9-20.

Sun, H., Niu, F., Zhang, K., Ge, X., 2017, Seismic behaviors of soil slope in permafrost regions using a large-scale shaking table. Landslides 14(4), 1-8.

Tang, C.A., Zuo, Y.J., Qin, S.F., 2008, Landslide shallow layer spalling cast modes and its kinetics explanation in Wenchuan earthquake. In: Song, S.W., (eds.), The proceedings of the tenth national rock mechanics and engineering science conference, Chengdu, China. pp 258-262. (In Chinese)

Ter-Stepanian, G., 1998, Suspension force induced landslides. Proceedings of 8th International Congress International Association for Engineering Geology and the Environment, Vancouver, Canada, 3.Balkema, Rotterdam, 1905-1912.

Wang, G., Zhang, D., Furuya, G., Yang, J., 2014, Pore-pressure generation and fluidization in a loess landslide triggered by the 1920 Haiyuan earthquake, China: a case study. Engineering Geology 174, 36-45.

Wang, K.L., Lin, M.L., 2011, Initiation and displacement of landslide induced by earthquake-a study of shaking table model slope test. Engineering Geology 122(1), 106-114.

Wang, W., 1979, Some Findings in Soil Liquefaction. Water Conservancy and Hydroelectric Power Scientific Research Institute, Beijing, China.

Wartman, J., Seed, R.B., Bray, J.D., 2005, Shaking table modeling of seismically induced deformations in slopes. Journal of Geotechnical and Geoenvironmental Engineering 131(5):, 610-622.

Xie, Y.S., Cai, M.B., 1983, Compilation of Historical Materials of Chinese Earthquakes, From Remote Antiq. to the Yuan Dynasty, vol. 1, Science, Beijing. (In Chinese).

Xie, Y.S., Cai, M.B., 1985, Compilation of Historical Materials of Chinese Earthquakes, The Ming Dynasty, vol. II, Science, Beijing. (In Chinese).

Xie, Y.S., Cai, M.B., 1987a, Compilation of Historical Materials of Chinese Earthquakes, The Qing Dynasty-1, vol. III, Science, Beijing. (In Chinese).

Xie, Y.S., Cai, M.B., 1987b, Compilation of Historical Materials of Chinese Earthquakes, The Qing Dynasty-2, vol. III, Science, Beijing. (In Chinese).

Xu, C., Xu, X., Yu, G., 2013, Landslides triggered by slipping-fault-generated earthquake on a plateau: an example of the 14

April 2010, Ms 7.1, Yushu, China earthquake. Landslides 10(4), 421-431.

Xu, Q., Zhang, S., Li, W., 2011, Spatial distribution of large-scale landslides induced by the 5.12 Wenchuan earthquake. Journal of Mountain Science 8(2), 246-260.

Xu, Z.J., Lin, Z.G., Zhang, M.S., 2007, Loess in china and loess landslides. Chinese Journal of Rock Mechanics and Engineering 26(7), 1297-1312. (in Chinese)

Yin, Y., Wang, F., Sun, P., 2009, Landslide hazards triggered by the 2008 Wenchuan earthquake, Sichuan, China. Landslides 6(2), 139-152.

Zhang, D., Wang, G., 2007, Study of the 1920 Haiyuan earthquake-induced landslides in loess (China).Engineering Geology 94(1), 76-88.

Zhang, D., Wang, G., 2007, Study of the 1920 Haiyuan earthquake-induced landslides in loess (China). Engineering Geology 94(1), 76-88.

Zhang, D., Wang, G., Luo, C., Chen, J., Zhou, Y., 2009, A rapid loess flowslide triggered by irrigation in China.Landslides 6(1), 55-60.

Zhang, M., Yin, Y.P., 2013, Dynamics, mobility-controlling factors and transport mechanisms of rapid long-runout rock avalanches in China. Engineering Geology. 167(1), 37-58.

Zhang, P.Z., Molnar, P., Burchfiel, B.C., Royden, L., Zhang, W., Jiao, D., Deng, Q., Wang, Y., Song, F., 1988a, Bounds on the recurrence interval of major earthquakes along the Haiyuan fault in north-central China, Seismol. Res. Lett. 59, 81-89.

Zhang, P.Z., Molnar, P., Burchfiel, B.C., Royden, L., Zhang, W., Jiao, D., Deng, Q., Wang, Y., Song, F., 1988a, Bounds on the Holocene slip ratealong the Haiyuan Fault, north-central China, Quat. Res. 30, 151-164.

Zhang, W. Q., Jiao, D.C., Zhang, P.Z., Peter, M., Burchfield, B.C., Deng, Q.D., Wang, Y.P., Song, F.M., 1987, Displacement along the Haiyuan fault associated with the great 1920 Haiyuan, China, earthquake. Bulletin of the Seismological Society of America 77(1), 117-131. (In Chinese)

Zhang, X.B., Higgitt, D.L., Walling, D.E.,1991, A preliminary assessment of the potential for using caesium-137 to estimate rates of soil erosion in the loess plateau of china. Geochimica 35(3), 243-252.

Zhang, Z., Wang, L., 1995, Geological disasters in loess areas during the 1920 Haiyuan Earthquake, China. GeoJournal 36(2-3), 269-74.

Zhuang, J., Cui, P., Hu, K., Chen, X., Ge, Y., 2010, Characteristics of earthquake-triggered landslides and post-earthquake debris flows in Beichuan County. Journal of Mountain Science 7(3), 246-254.

Zhuang, J.Q., Peng, J.B., Wang, G.H., Javed, I., Wang, Y., Li W., Xu, Q., Zhu, X.H., 2017, Prediction of rainfall- induced shallow landslides in the Loess Plateau, Yan'an, China, using the TRIGRS model. Earth Surface Processes and Landforms 42(6), 915-927.

Tables:

Table 1 The sizes and numbers of landslides triggered by earthquakes in recent years

Table 2 Physical parameters of the loess in Xiji County

Table 1 The sizes and numbers of landslides triggered by earthquakes in recent years

Items	Study area (km^2)	Number of landslides	Landslide areas(km^2)	Average landslide area(km^2)
Northridge earthquake (Harp and Jibson, 1996)	10,000	11,111	23.8	0.00214
Haiyuan Earthquake	40,000	3,700	117.5	0.03162
Wenchuan Earthquake (Dai et al., 2011)	41,750	56,000	811.0	0.01448
Chi-Chi earthquake (Lin and Tung, 2004)	--	9,297	128.0	0.01374
Kashmir earthquake (Owen et al., 2008)	7,500	2,424	--	--

Table 2 Physical parameters of the loess in Xiji County

Items	Particle size/ % <0.005 mm	Particle size/ %0.005-0.075 mm	W_P /%	W_L / %	W_C /%	W_S /%	W_S/W_L
Sample 1	13.90	80.99	20.00	28.70	11.60	36.00	1.25
Sample 2	13.02	81.30	20.20	28.50	14.30	39.00	1.37
Sample 3	14.67	83.30	21.80	28.20	14.20	36.00	1.27

W_P is the water content;S_R is the saturation rate.

Figures:

Highlights:

The landslides distribution was not symmetrical around the fault.

Landslides induced by the Haiyuan Earthquake were clustered near ridge crests.

Slope aspects facing away from the direction of movement of the block were more susceptible to landslides.

The loess landslides move greater distances than rock landslides triggered by earthquakes.

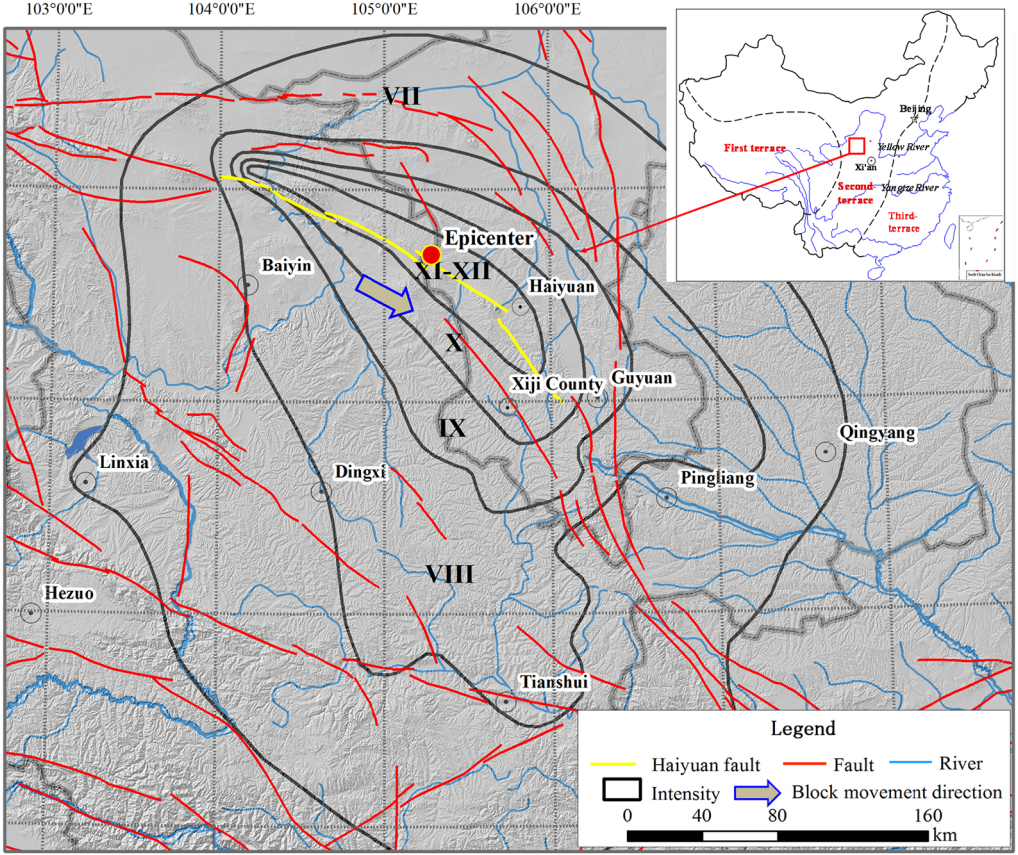
103°0'0"E
104°0'0"E
105°0'0"E
106°0'0"E
107°0'0"E
108°0'0"E
37°0'0"N
36°0'0"N
35°0'0"N
34°0'0"N
VII
Epicenter
XI-XII
Baiyin
Haiyuan
X
Xiji County
Guyuan
IX
Qingyang
Linxia
Dingxi
Pingliang
VIII
Hezuo
Tianshui
Beijing
First terrace
Yellow River
Xi'an
Second terrace
Yangtze River
Third terrace
Legend
Haiyuan fault
Fault
River
Intensity
Block movement direction
0
40
80
160
km

Figure 1

Figure 2

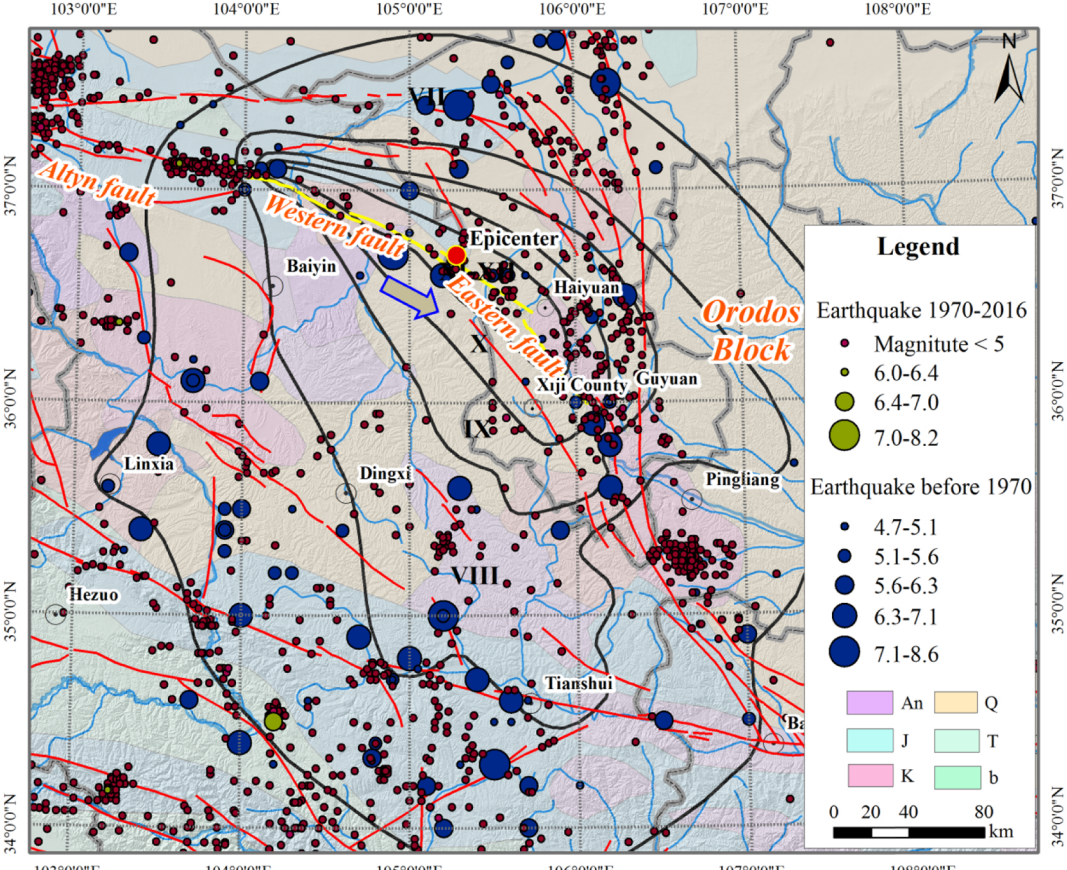
103°0'0"E
104°0'0"E
105°0'0"E
106°0'0"E
107°0'0"E
108°0'0"E
37°0'0"N
36°0'0"N
35°0'0"N
34°0'0"N
N
Altyn fault
Western fault
Eastern fault
Epicenter
Baiyin
Haiyuan
Orodos Block
Xiji County
Guyuan
Linxia
Dingxi
Pingliang
Hezuo
Tianshui
VII
VIII
IX
X
XI
Legend
Earthquake 1970-2016
Magnitute < 5
6.0-6.4
6.4-7.0
7.0-8.2
Earthquake before 1970
4.7-5.1
5.1-5.6
5.6-6.3
6.3-7.1
7.1-8.6
An
Q
J
T
K
b
0 20 40 80
km

Figure 3

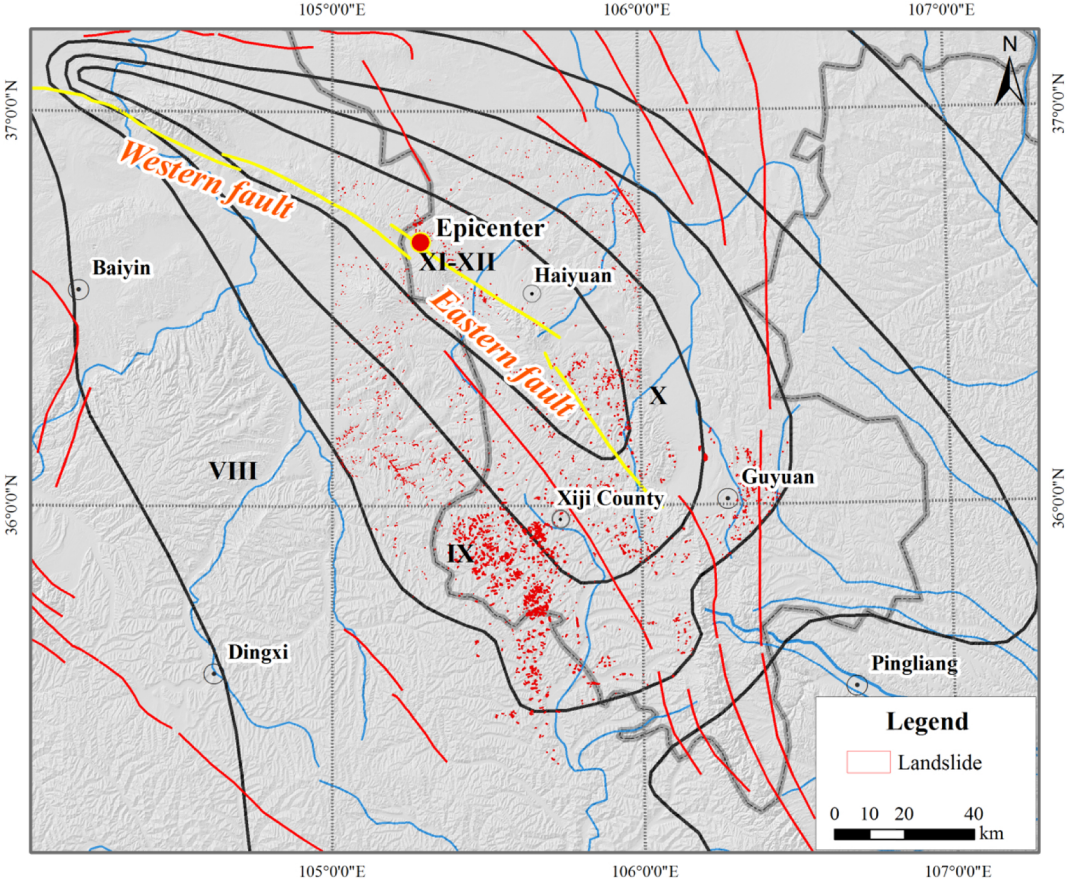
105°0'0"E
106°0'0"E
107°0'0"E
37°0'0"N
36°0'0"N
N
Western fault
Epicenter
XI-XII
Haiyuan
Eastern fault
X
Baiyin
VIII
Guyuan
Xiji County
IX
Dingxi
Pingliang
Legend
Landslide
0 10 20 40
km

Figure 4

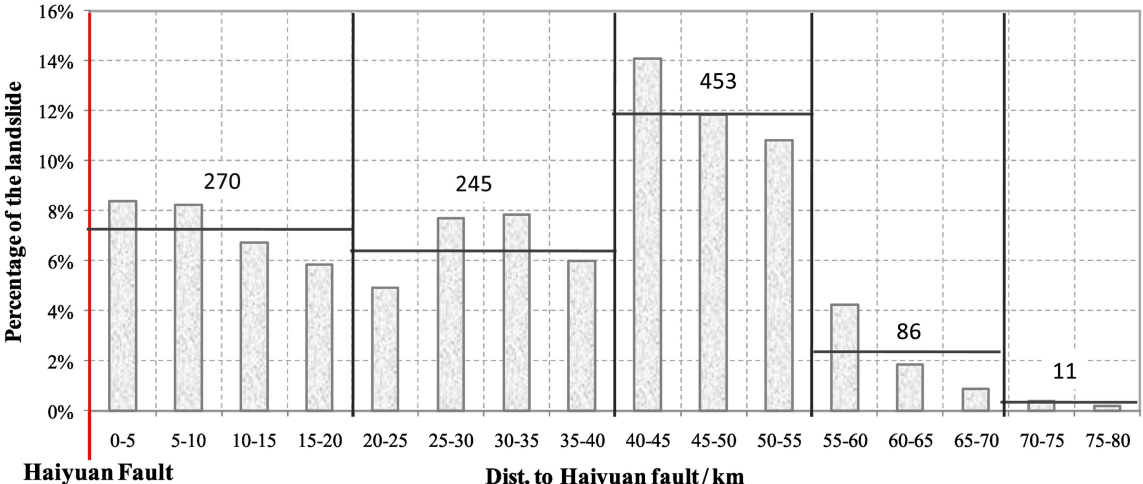
16%
14%
12%
10%
8%
6%
4%
2%
0%
Percentage of the landslide
270
245
453
86
11
0-5
5-10
10-15
15-20
20-25
25-30
30-35
35-40
40-45
45-50
50-55
55-60
60-65
65-70
70-75
75-80
Haiyuan Fault
Dist. to Haiyuan fault / km

Figure 5

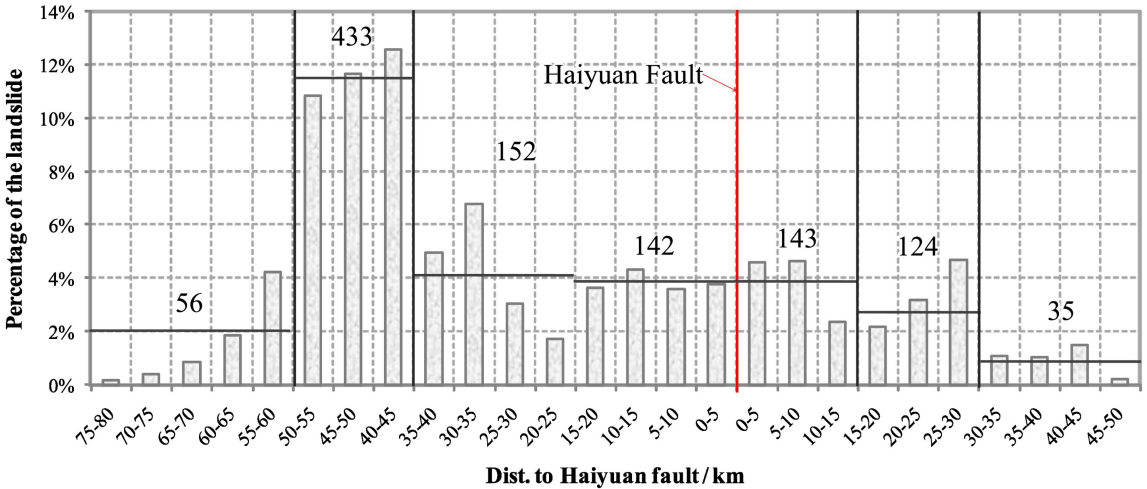
14%
12%
10%
8%
6%
4%
2%
0%
Percentage of the landslide
433
Haiyuan Fault
152
142
143
124
56
35
75-80
70-75
65-70
60-65
55-60
50-55
45-50
40-45
35-40
30-35
25-30
20-25
15-20
10-15
5-10
0-5
0-5
5-10
10-15
15-20
20-25
25-30
30-35
35-40
40-45
45-50
Dist. to Haiyuan fault / km

Figure 6

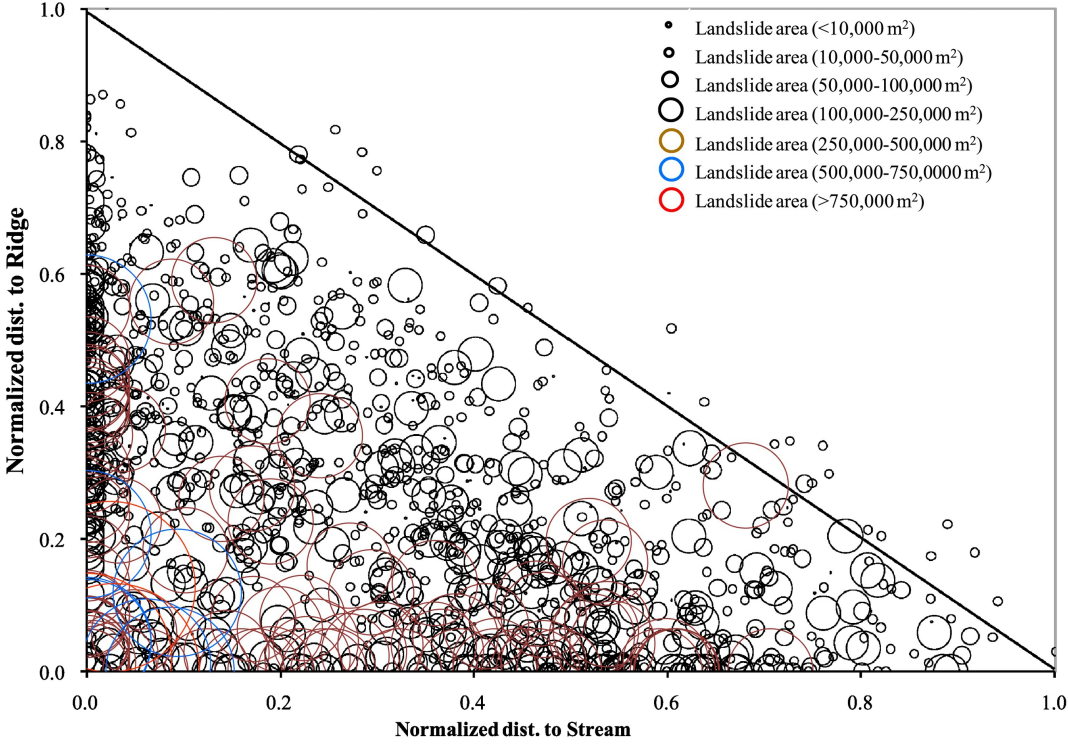
Landslide area (<10,000 m²)
Landslide area (10,000-50,000 m²)
Landslide area (50,000-100,000 m²)
Landslide area (100,000-250,000 m²)
Landslide area (250,000-500,000 m²)
Landslide area (500,000-750,0000 m²)
Landslide area (>750,000 m²)
Normalized dist. to Ridge
Normalized dist. to Stream
0.0
0.2
0.4
0.6
0.8
1.0

Figure 7

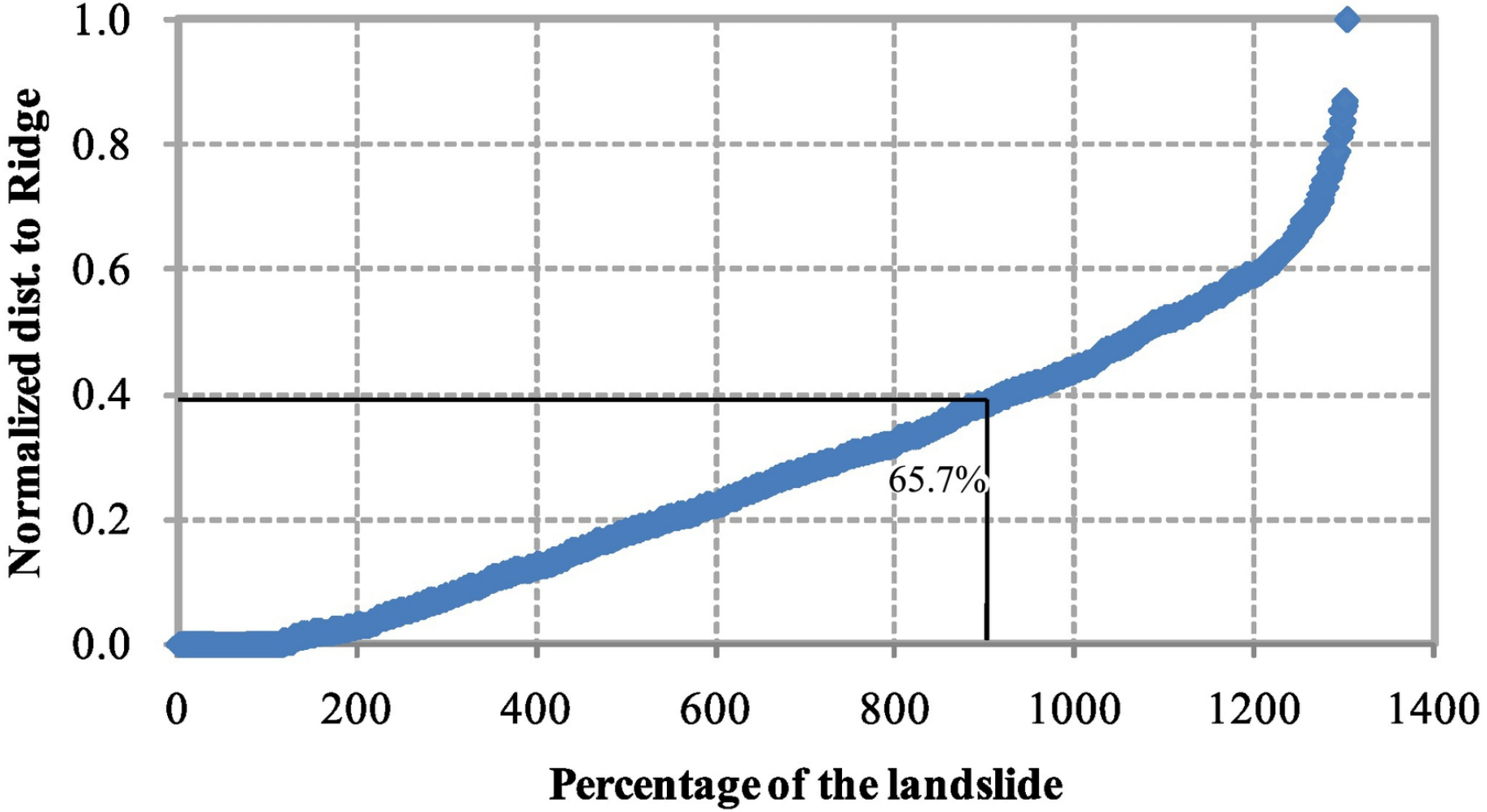
1.0
0.8
0.6
0.4
0.2
0.0
Normalized dist. to Ridge
65.7%
0
200
400
600
800
1000
1200
1400
Percentage of the landslide

Figure 8

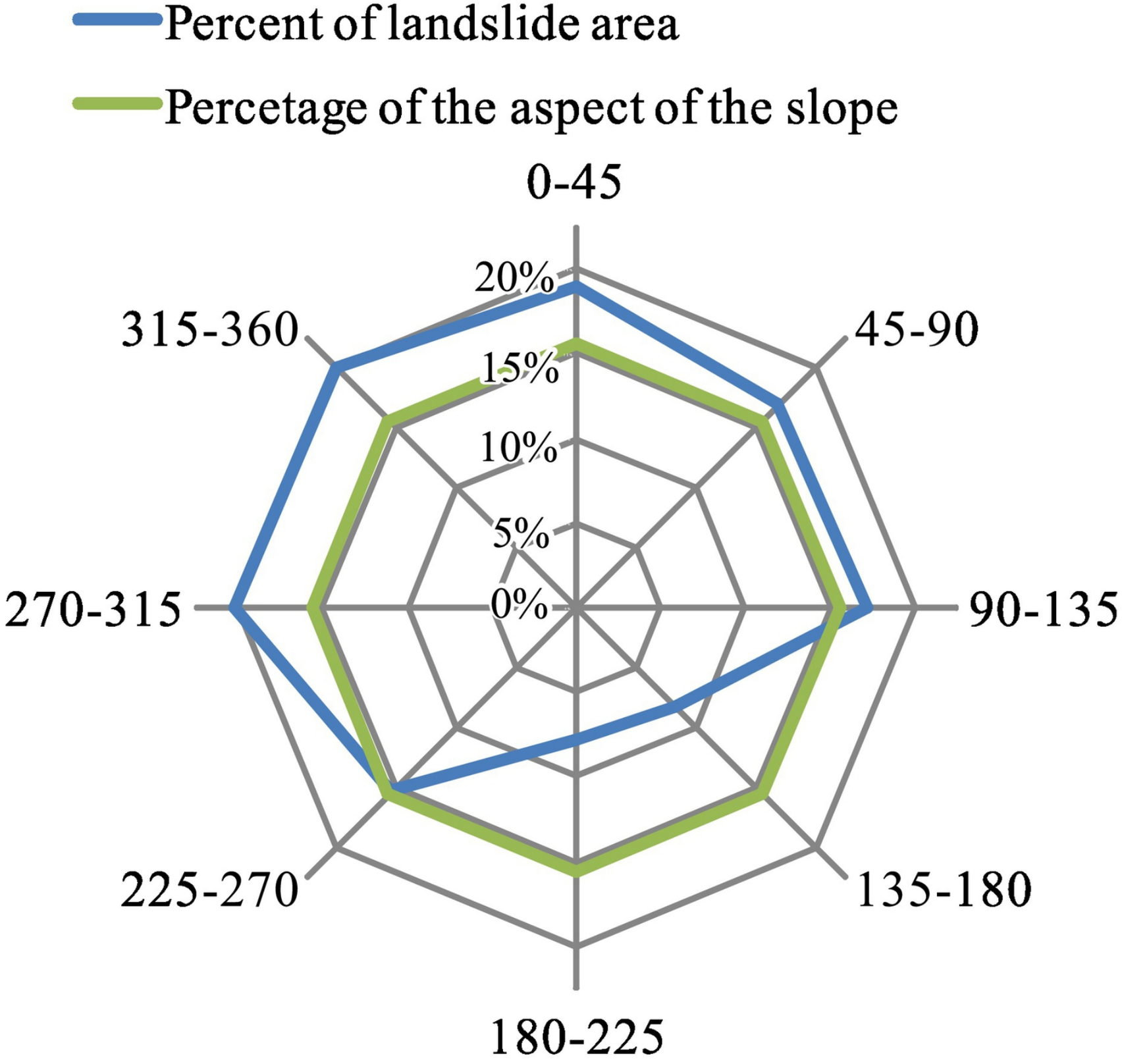
Percent of landslide area
Percetage of the aspect of the slope
0-45
45-90
90-135
135-180
180-225
225-270
270-315
315-360
20%
15%
10%
5%
0%

Figure 9

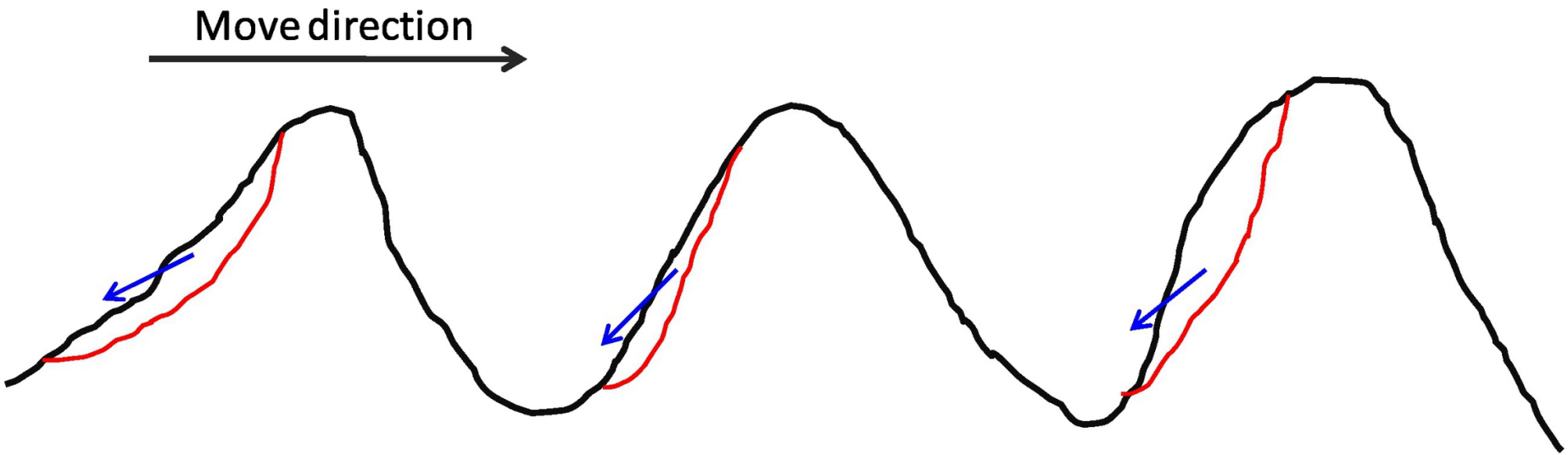

Figure 10

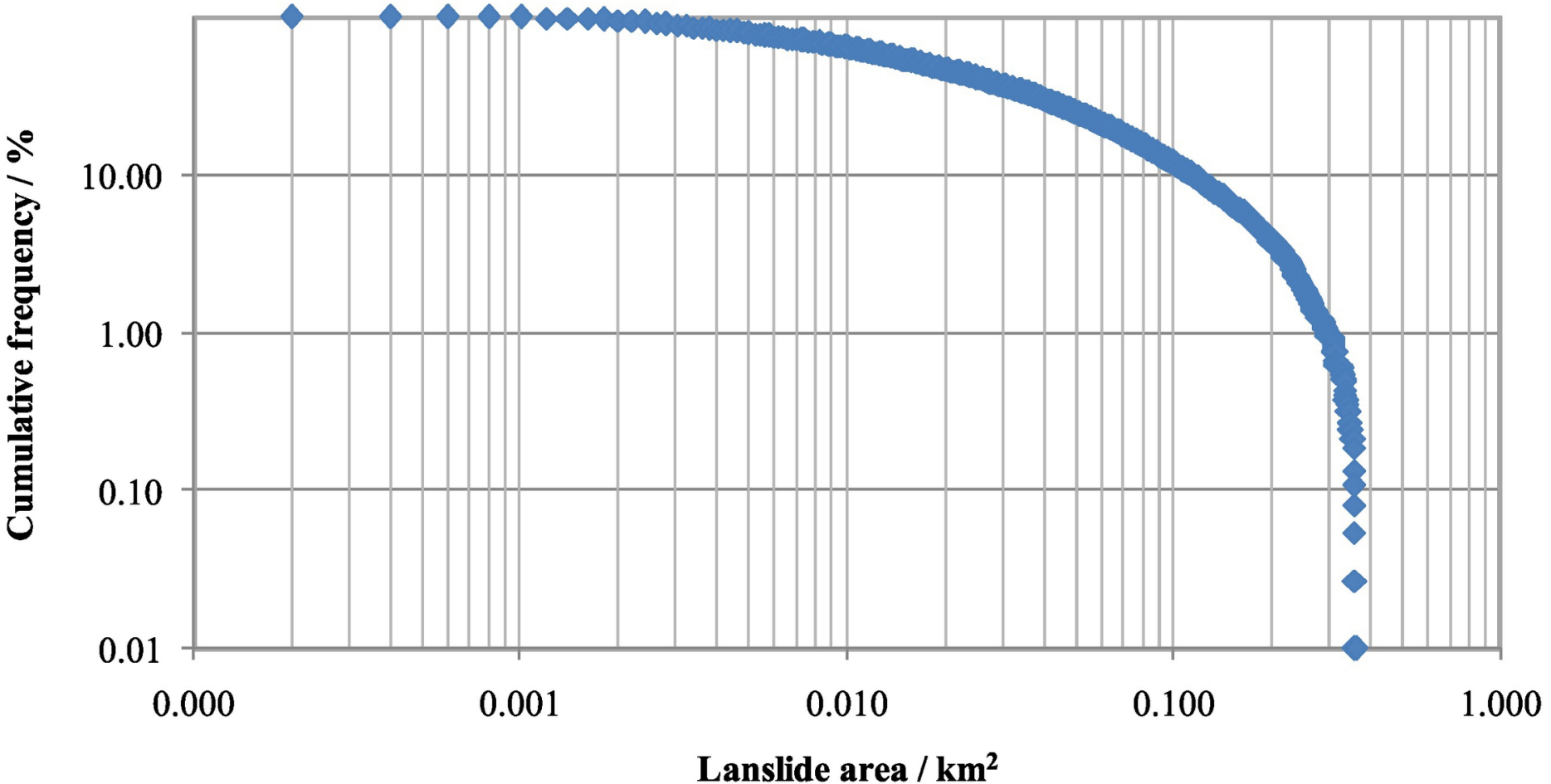
Cumulative frequency / %
10.00
1.00
0.10
0.01
0.000
0.001
0.010
0.100
1.000
Lanslide area / km²

Figure 11

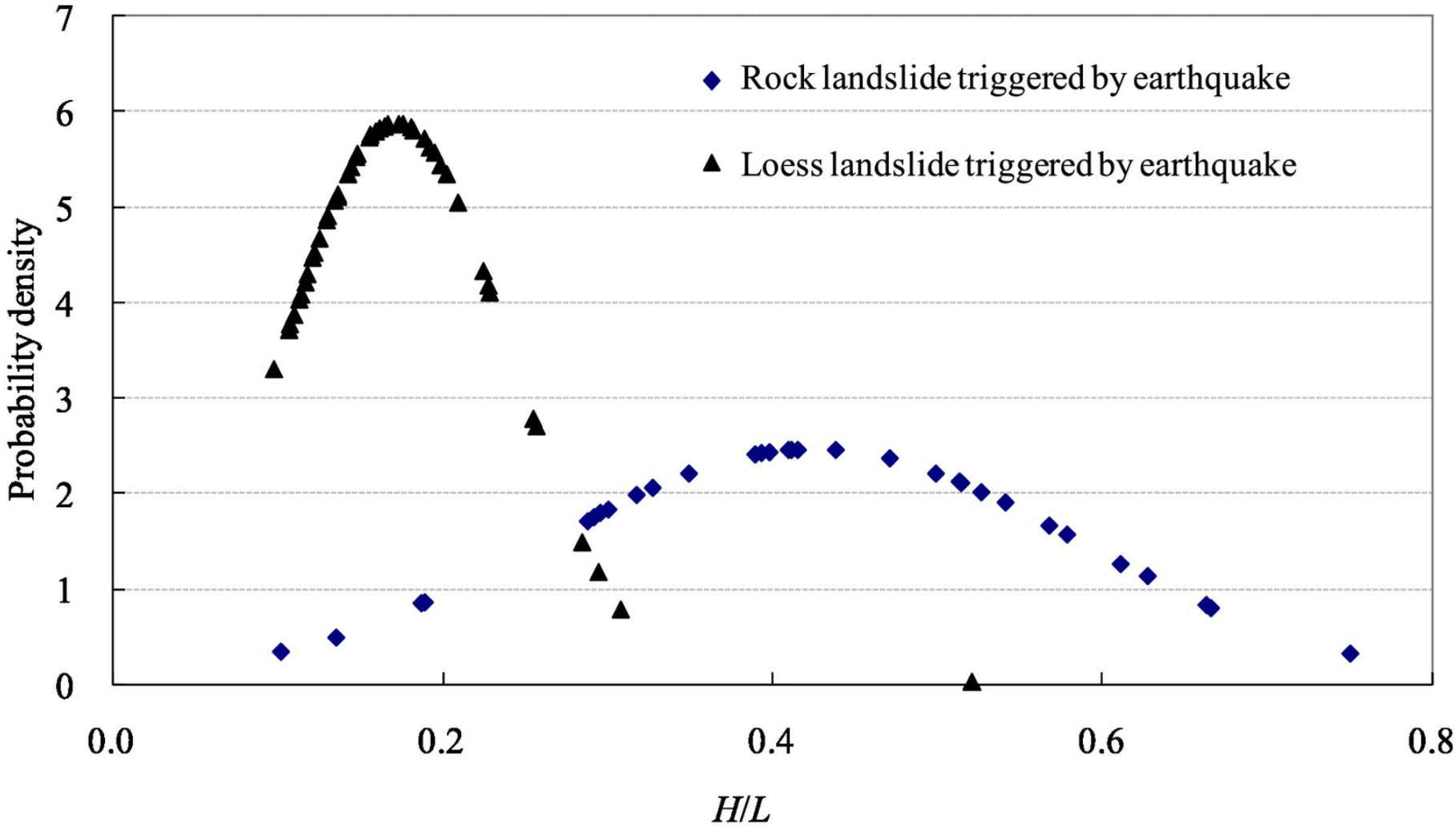
Rock landslide triggered by earthquake
Loess landslide triggered by earthquake
Probability density
H/L
0
1
2
3
4
5
6
7
0.0
0.2
0.4
0.6
0.8

Figure 12

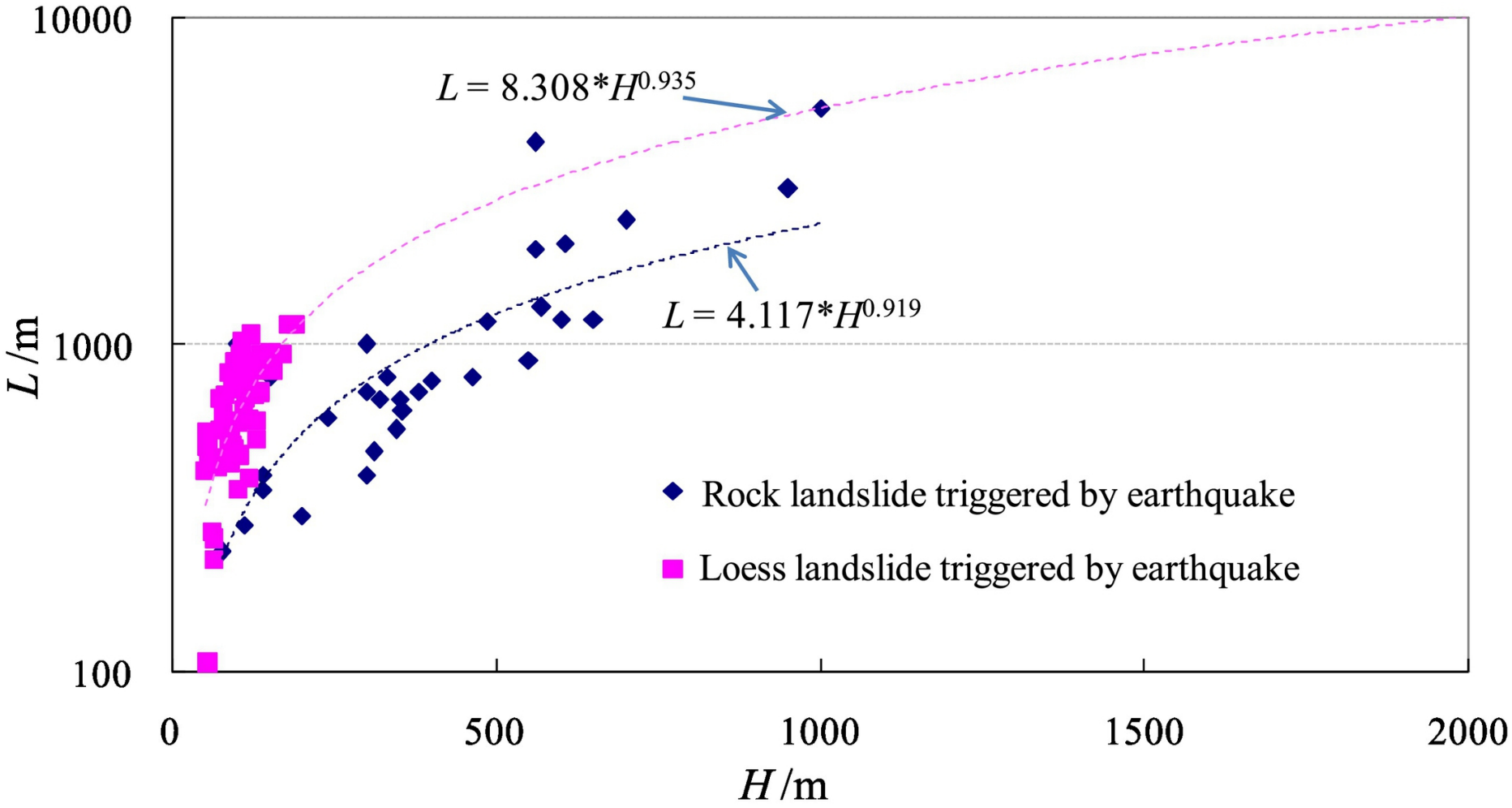
10000
1000
100
L /m
0
500
1000
1500
2000
H /m
L = 8.308*H^0.935
L = 4.117*H^0.919
Rock landslide triggered by earthquake
Loess landslide triggered by earthquake

Figure 13

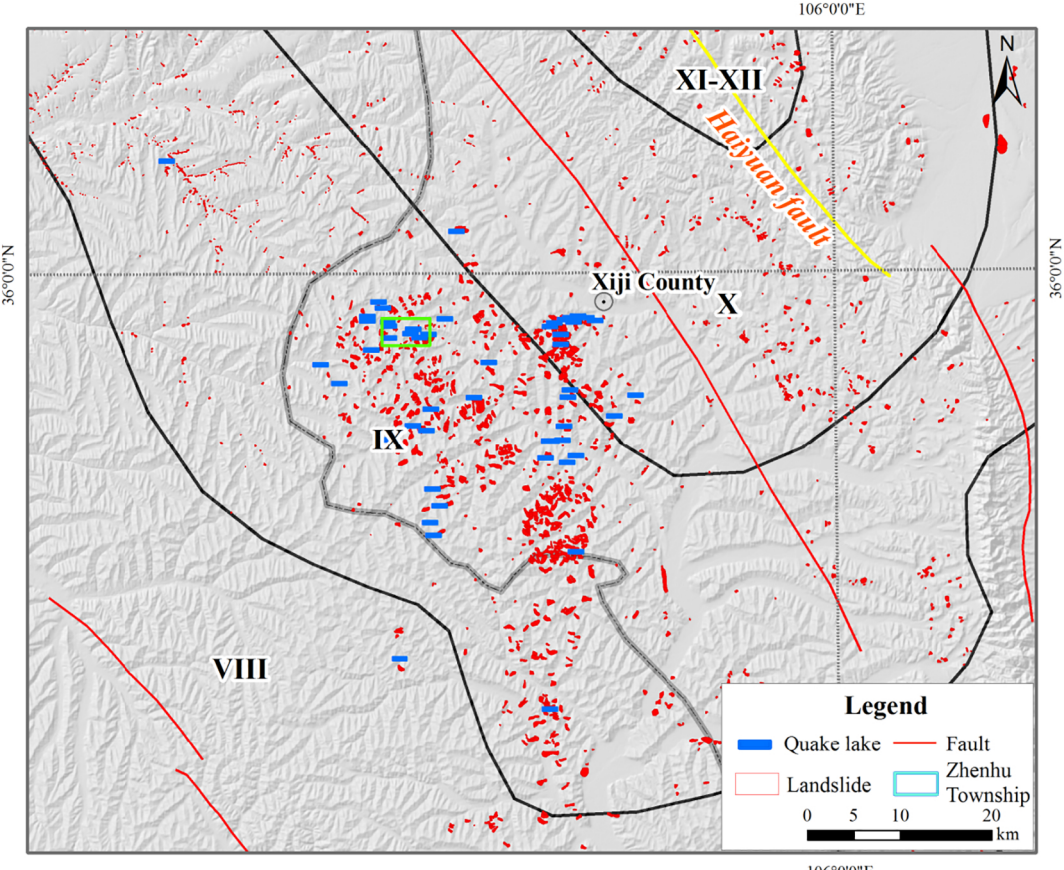
106°0'0"E
N
XI-XII
Haiyuan fault
36°0'0"N
Xiji County
X
IX
VIII
Legend
Quake lake
Fault
Landslide
Zhenhu Township
0 5 10 20
km
106°0'0"E

Figure 14

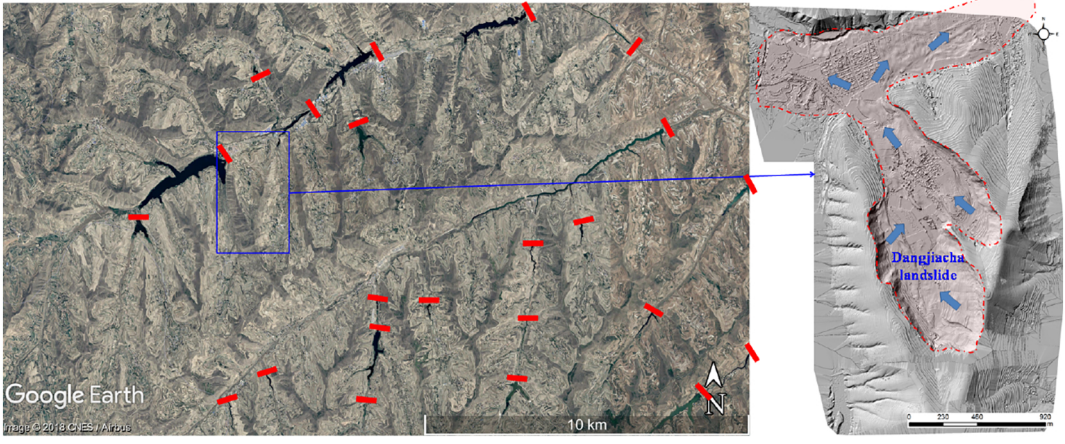
Google Earth
Image © 2018 CNES / Airbus
10 km
N
Dangjiacha landslide
0 230 460 920

Figure 15

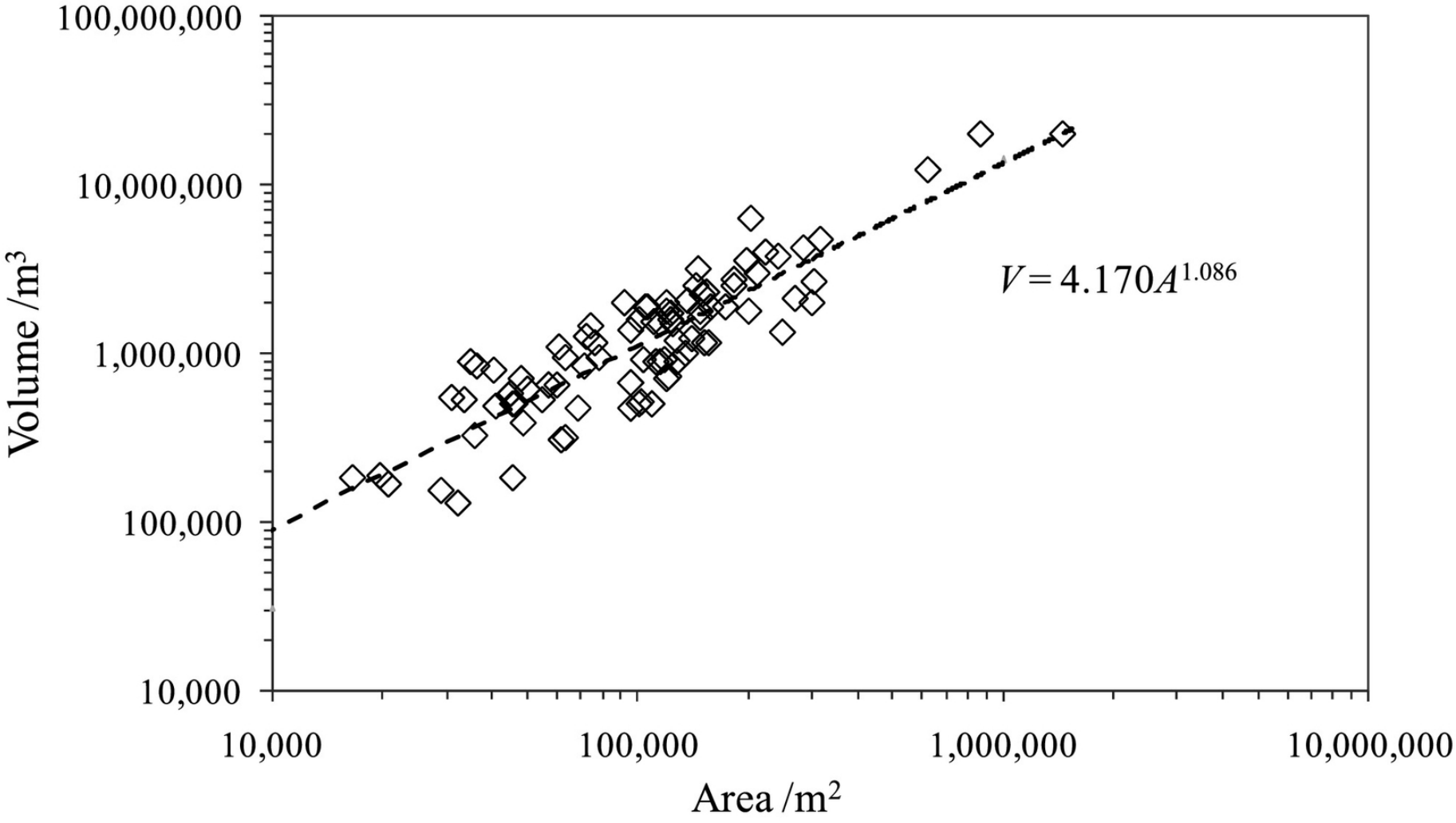
100,000,000
10,000,000
1,000,000
100,000
10,000
Volume /m3
10,000
100,000
1,000,000
10,000,000
Area /m2
V = 4.170A1.086

Figure 16

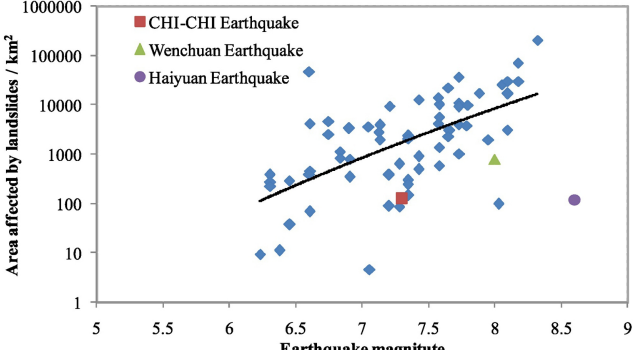
CHI-CHI Earthquake
Wenchuan Earthquake
Haiyuan Earthquake
Area affected by landslides / km²
1000000
100000
10000
1000
100
10
1
5
5.5
6
6.5
7
7.5
8
8.5
9
Earthquake magnitute

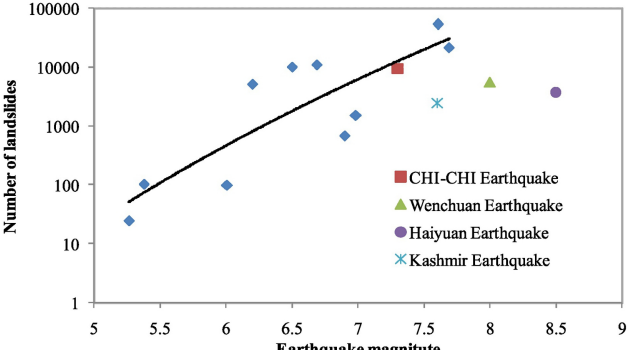
Number of landslides
100000
10000
1000
100
10
1
CHI-CHI Earthquake
Wenchuan Earthquake
Haiyuan Earthquake
Kashmir Earthquake
5
5.5
6
6.5
7
7.5
8
8.5
9
Earthquake magnitute

Figure 17

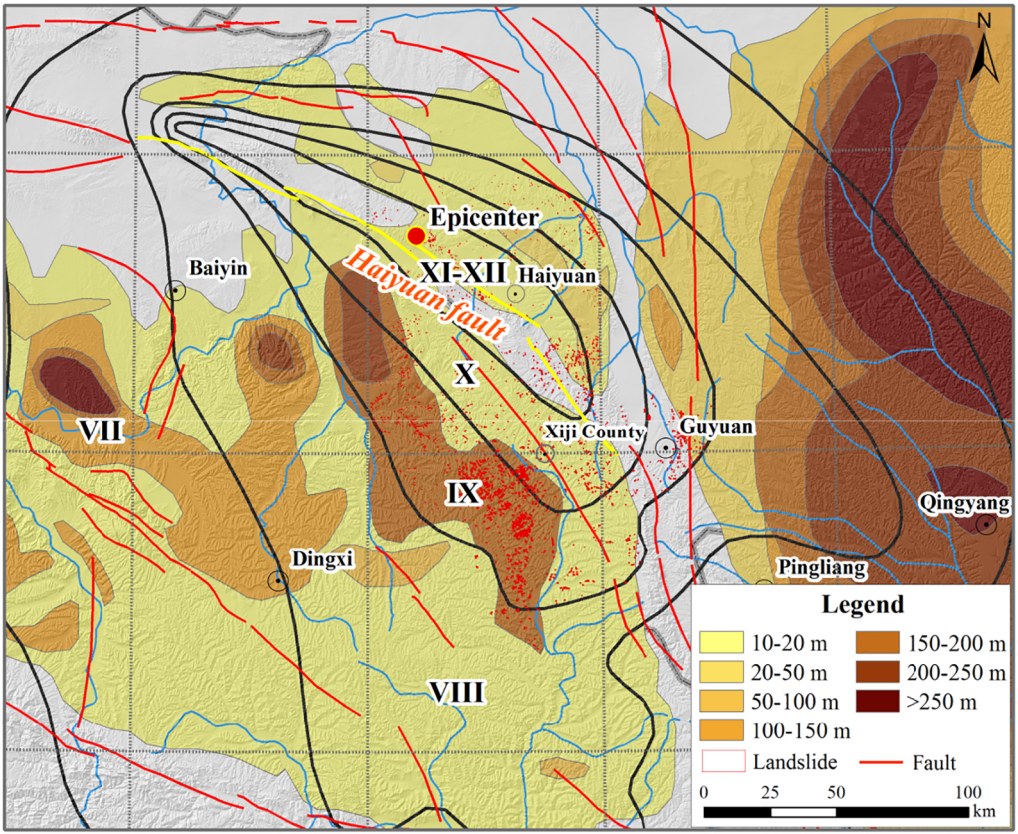
104°0'0"E
105°0'0"E
106°0'0"E
107°0'0"E
37°0'0"N
36°0'0"N
35°0'0"N
N
Epicenter
Haiyuan fault
XI-XII
Haiyuan
Baiyin
X
VII
Xiji County
Guyuan
IX
Qingyang
Dingxi
Pingliang
VIII
Legend
10-20 m
20-50 m
50-100 m
100-150 m
150-200 m
200-250 m
>250 m
Landslide
Fault
0
25
50
100
km

Figure 18